Experimental Investigation of Hydraulic Effects of Two-Stage Fuel Injection on Fuel Injection System and Diesel Combustion in a High-Speed Optical CR Diesel Engine

Mohammad Reza Herfatmanesh* **and Hua Zhao**

Centre for Advanced Powertrain and Fuels Research, School of Engineering and Design, Brunel University London, UK

**Corresponding author: Brunel University London, Uxbridge, London UB8 3PH. email: Mohammad.reza.herfatmanesh@brunel.ac.uk*

Abstract: In order to meet the ever more stringent emission standards, significant efforts have been devoted to the research and development of internal combustion engines. The requirements for more efficient and responsive diesel engines have led to the introduction and implementation of multiple injection strategies. However, the effects of such injection modes on the hydraulic systems, such as the high pressure pipes and fuel injectors, must be thoroughly examined and compensated for since the combustion and the formation of pollutants in direct injection engines are directly influenced by the spatial and temporal distribution of the injected fuel within the combustion chamber. This study investigated the hydraulic effects of two-stage fuel injection on diesel combustion and emissions. The fuel injection system was characterised for all the tested strategies through the measurement of the fuel injection rate and quantity. In particular, the interaction between the two injection events was identified. The effects of two-stage injection, dwell angle and the interactions between two consecutive injection events on the combustion process and the emissions were investigated in a high-speed direct injection single cylinder optical diesel engine using heat release analysis and high speed fuel spray and combustion visualisation technique. The results indicated that two-stage injection strategy has the potential for simultaneous reduction of NOx, soot and uHC emissions. The results suggested that an optimum fuel quantity in the first injection exists, 0-30%, with which simultaneous reduction of NOx, soot and uHC emissions can be achieved with the added benefits of improved engine performance, fuel economy and combustion noise. However, higher soot emissions were produced, mainly due to the interaction between the two consecutive fuel injection events whereby the fuel sprays during the second injection were injected into burning regions, as well as reduced soot oxidation due to the continuation of the combustion into the expansion stroke.

Keywords: diesel engine, injection rate, two-stage injection, dwell angle, emissions

1 INTRODUCTION

A significant cost of industrialisation has been the environmental damages inflicted, to a large extent by the use of fossil fuels, within which the significant growth in the use and production of internal combustion (IC) engines have since been considered as one of the primary contributing factors. Due to ever increasing concern over the environmental impacts of the exhaust pollutants, emissions legislations have been progressively enforced since the 1960s. Diesel engines have long been the power plant of choice whether for transportation or industrial applications. However, inherent high levels of regulated and unregulated emissions and combustion noise associated with conventional diesel engines have been the foremost reasons for relatively low market share until the late 1990s. Though, recent developments in diesel engine technology, higher fuel prices as well as incentivising tax regimes based on CO_2 emission levels have led to a substantial shift in the automotive market with diesel engines claiming approximately 50% of the European car market [**1**].

In order to comply with the current and future emissions legislations, the development of more effective, responsive and environmentally-friendly combustion systems is essential. There are several ways of tackling this problem such as the design and development of advanced fuel injection and combustion systems and/or exhaust gas after-treatment. Nevertheless, the most beneficial solution is to tackle the problem at source through the use of sophisticated fuel injection and combustion systems, capable of meeting the requirements over the complete range of engine operating conditions. In direct injection (DI) diesel engines, the combustion and the formation of pollutants are directly influenced by the spatial and temporal distribution of the fuel injected into the combustion chamber. Consequently, numerous research studies have been carried out aimed at more detailed investigation of fuel-air mixing and combustion processes as well as chemical/physical reactions involved in the production of pollutants, in particular nitrogen oxides (NOx) and particulate matter (PM), the two most perilous emissions produced by diesel engines.

The introduction of the common rail (CR) fuel injection system in the 1990s allowed greater control and flexibility on the fuel injection pressure, rate, quantity and timing over the entire operating range of diesel engines. The initial studies involved detailed analysis of the effects of increased injection pressure on diesel combustion and the exhaust emissions. Although, significant reduction in soot emission due to improved fuel atomisation, evaporation and mixing was reported, increase in NOx emission was an inherent by-product. Even though, NOx production can be reduced by retarding the injection timing (i.e. decreasing peak in-cylinder pressure and temperature) and/or exhaust gas recirculation (EGR), penalties in terms of fuel economy and engine efficiency are ultimately incurred. Nevertheless, there are limitations on the maximum practical injection pressures mainly due to increased parasitic losses, material strength and increased fuel injection system cost [**2**]. Subsequent investigations revealed that the rate of fuel injection, a characteristic of a common rail diesel fuel injector, is a function of the injection pressure and the injection strategy utilised. The rate of fuel injection and its effect on engine noise, emission and performance has been extensively investigated since the early 1980s. Nehmer and Reitz [**3**] studied the effect of several injection rate profiles. Their result indicated that the combustion with injectors having slower rate profiles allowed the combustion to continue later in the expansion cycle. Although this resulted in reduction of soot emission through improved oxidation process, increase in fuel consumption was reported. Subsequently Tow et al. [**4**] investigated the effect of different dwell angles using the same engine. They reported on the potential for significant soot reduction with no increase in NOx emission and minor increase in fuel consumption under high load condition using two-stage fuel injection with relatively long dwell angle. Their result indicated that the control of soot production with the studied fuel injection strategy was highly dependent on the dwell angle utilised.

Zambare and Winterbone [**5**] used an optical engine in order to investigate the effect of injection rate profile of conventional and two-stage fuel injection equipments (FIE). Their result showed that NOx emission was reduced with the latter injection system in comparison to a conventional injection system, though soot emission was higher, particularly at low loads. Juneja et al. [**6**] investigated the effect of different injection rate profiles on liquid and vapour penetration, flame lift-off length and emissions characteristics. The injection rate profiles were defined based on extensive computational analysis of advanced fuel evaporation and primary jet breakup models which were further validated by experimental investigations. The results indicated that NOx and soot emissions were directly influenced by the equivalence ratio of the premixed fuel mixture prior to the onset of combustion which could be controlled through modification of injection rate profile. Thus, it was reported that regulation of fuel distribution in the combustion chamber through modification of injection rate profile plays an important role in controlling exhaust emissions. Tanabe et al. [**7**] developed a novel two-rail system comprising of a low and high pressure rail, feeding a single injector. The fuel injection rate was controlled by switching between the rails during fuel injection. The experiments were carried out in a heavy duty diesel engine. Their results showed that fuel injection rate shaping resulted in simultaneous reduction of NOx and soot emissions, particularly at mid speed and high loads where control over combustion led to a more constant pressure combustion process similar to an ideal diesel cycle. Although alternative combustion modes are also capable of simultaneous reduction of NOx and soot emissions, fuel injection rate shaping allows simultaneous reduction of the aforementioned pollutants with no penalty in terms of fuel economy.

The fuel injection timing, duration and pressure in CR fuel injection systems are independent of the engine speed; thus, capable of promoting improved fuel evaporation and mixture formation at low speeds and loads. In recent years, advancement in the design of such versatile and flexible systems has led to the development of alternative combustion modes including low temperature combustion (LTC) [**8**-**14**], homogeneous charge compression ignition (HCCI) [**14**-**22**], premixed charged compression ignition (PCCI) [**23**-**29**] and partially premixed combustion (PPC) [**30-33**] through the application of sophisticated fuel injection strategies. The results revealed the potential for simultaneous reduction of NOx and PM emissions through the application of such fuel injection and combustion modes. The initial investigations on using alternative injection strategies were primarily focused on the application of pilot and main injections or split injections with equal fuel demand per injection (50%/50%) [**2**, **3**, **34**]. The results demonstrated that shorter ignition delay was achieved due to pilot injection, indicating less premixed combustion, lowering the peak heat release rate. Therefore, NOx emission as well as combustion noise was considerably reduced in comparison to the conventional diesel combustion. In addition, the effect of post injection on further reduction of soot emission was examined by Han et al. [**35**] and Farrell et al. [**36**]. Their results showed that soot emission was reduced due to improved soot oxidation which was attributed to higher combustion temperature during mixing controlled combustion phase caused by the combustion of fuel injected during post injection. Furthermore, the potential for further reduction of exhaust emissions using EGR has been extensively investigated. Montgomery and Reitz [**37**] studied the effect of EGR in a heavy duty diesel engine using 50%/50%, 55%/45% and 70%/30% split injection strategies with EGR levels varying between 10% to 25%. Their investigation revealed the potential for simultaneous reduction of NOx and soot emissions using split injection with EGR. The use of EGR decreased the NOx emission by limiting the peak heat release rate due to premixed combustion, thus lowering the in-cylinder temperature. The soot emission was reduced due to improved mixing in conjunction with the effect of late fuel injection which resulted in higher in-cylinder temperatures during diffusion combustion, maximising soot oxidation. In order to better understand the mixing process, Zhang et al. [**38**] carried out a series of investigations involving detailed analysis of fuel-air mixing process in a constant volume vessel through the application of laser absorption scattering (LAS). They investigated the mixing process using conventional single injection and compared their results with those obtained through split injection strategies 75%/25%, 50%/50% and 25%/75%. It was reported that the 75%/25% split injection strategy resulted in maximum soot reduction under the tested engine operating conditions. This was mainly attributed to improved mixing due to increased in-cylinder turbulence caused by the combustion of fuel injected during the second injection. The influence of pilot injection has also been investigated by Carlucci et al. [**39**, **40**]. Their result indicated that small quantity of fuel injected during pilot injection results in shorter ignition delay thus lowering the level of NOx emissions. However, increasing trend of particulate emissions with increasing pilot injected fuel at lower engine speeds was observed while the opposite behaviour was found at higher engine speeds. Shayler et al. [**41**] also compared the combustion and emissions characteristics of single and split injections in a light duty diesel engine. In this study all the split injection strategies were accompanied by a pilot injection whereby relatively small quantity of fuel was injected in order to improve fuel evaporation during split-main injections. The results indicated that strategies with more fuel quantity during the first injection resulted in less soot emission with no increase in NOx emission.

Koyanagi et al. [**42**] investigated the effects of engine design and operation parameters, in particular injector stability, spray symmetry, nozzle geometry, injection rate, pilot injection and swirl effects, in a light duty single cylinder optical diesel engine with similar production-type combustion chamber geometry. The authors reported that the pilot-main strategy was characterised by a complete premixed combustion of the fuel injected during the pilot injection, 10% of the total injected fuel quantity in this case. Therefore, ignition delay time was reduced due to increased in-cylinder pressure and temperature and the presence of active radical. Consequently higher soot emission was produced due to deteriorated mixing of the main injected fuel; however, such an effect could be controlled through the use of a suitable dwell angle. Badami et al. [**43**] also investigated the effect of pilot injection quantity and dwell angle on diesel combustion and emissions in a light duty diesel engine. In this study, the effects of pilot injection less than 1% to 15% of the total injected fuel quantities were investigated. It was reported that soot and NOx emissions increased as the quantity of the pilot injection increased. The former was attributed to the increase in the in-cylinder pressure and temperature, due to the main combustion advance, while the latter was ascribed to the reduction of the premixed combustion. The same trend was observed as the dwell angle was reduced. The authors also reported on the hydraulic effects of pilot injection on the combustion characteristics and the fluid-dynamic conditions at the start of the main injection.

Schmid et al. [**44**] investigated the effect of nozzle hole geometry, rail pressure and pre-injection in a single cylinder transparent light duty diesel engine. The authors reported that the pre-injection (i.e. pilot) could lead to shorter ignition delay which in turn could result in the penetration of the main injection into burning regions. Kook and Bae [**45**] investigated the effect of two-stage fuel injection in a single cylinder DI PCCI engine. In this study the majority of the fuel was injected early during the first injection to form the premixed charge while a small quantity of fuel was injected close to TDC, serving as the ignition promoter. The results indicated that simultaneous reduction in emissions as well as improved combustion efficiency can be achieved provided that a combination of optimised fuel quantity, intake air temperature, injection pressure and compression ratio was used. Horibe et al. [**46**] investigated the effect of pilot-main fuel injection quantity ratio and dwell angle in a constant volume vessel under simulated partial PCCI conditions using two-stage injection. They reported that in the case of small first injection quantity, longer dwell angle reduced the initial peak heat release rate while the opposite was observed for shorter dwell angles whereby the second fuel injection suppressed the ignition of the mixture from the first injection, thus, increasing the amount of combustible mixture at the time of ignition. However, in the case of larger first injection quantity, the peak of the initial heat release rate was not controlled by the dwell angle since the second injection took place in a high temperature environment due to the combustion of the fuel injected during the first injection. Nevertheless, under low ambient oxygen mole fraction (i.e. two-stage with EGR), the dwell angle influenced the peak heat release rate since the ignition of the fuel injected during the first injection was delayed due to larger fuel quantities injected.

Although, the hydraulic effects of two-stage fuel injection has been previously reported [**47**-**51**], the effects of advanced fuel injection modes on the fuel injection system are yet to be fully explored and few detailed in-cylinder studies have been carried out on the interaction of two-stage fuel injection and their effect on the injected fuel quantity, combustion characteristics and exhaust emissions. The objective of this study is to investigate the hydraulic effects of two-stage fuel injection on diesel combustion and emissions. The 30%/70%, 50%/50% and 70%/30% two-stage injection strategies were investigated in a single cylinder direct injection high-speed optical diesel engine by means of conventional heat release analysis and high speed fuel spray and combustion visualisation technique. In order to quantify the interactions between the two consecutive fuel injection events in the solenoid CR fuel injector, a fuel injection characterisation rig and fuel bulk modulus measurement device were commissioned and applied. Therefore, in the first part of the paper, the principle and application of the fuel injection rate and bulk modulus measurement techniques are presented. Then the experimental setup and in-cylinder measurement techniques are described. Effects of two-stage fuel injection and the interactions of two consecutive injection events on the combustion process and pollutant formation are then presented and discussed.

2 FIE CHARACTERISATION

In this study, a fuel injection rate characterisation rig was commissioned in order to study the effects of multiple injection and alternative diesel fuels on the performance of CR fuel injection system.

2.1 Principle

The evaluation method employed in this study was based on the Zeuch's method presented by Ishikawa et al. [**52**]. The principle of this technique is based on the injection of fuel into a constant volume chamber (CVC) filled with the selected fuel for the measurements, in this case commercially available diesel fuel. Consequently, the pressure inside the chamber increases, this augmentation is proportional to the quantity of fuel injected. Therefore, the rise in pressure (ΔP) can be determined by the following expression as a function of the change in volume (ΔV),

$$\Delta P = k\frac{\Delta V}{V} \qquad (1)$$

Where k bulk modulus of fuel

V total volume of the chamber

The fuel injection rate can be determined by differentiating equation (1) with respect to time (t) as depicted below,

$$\frac{dV}{dt} = \frac{V}{k}\times\frac{dP}{dt} \qquad (2)$$

In the case of a single injection, fuel quantity and injection duration as a function of injection pulse width could be measured through the application of this technique. In addition, interference between injections could also be identified for two-stage or multiple injections, whereby substantial variations in the quantity and rate of fuel injection could be experienced.

Although the Bosch rate of injection meter has been widely used as the standard measurement tool, the Zeuch's method was selected for the purpose of this investigation due to its greater accuracy at predicting the injected volume [**53**]. Nevertheless, both systems predict the same magnitude and shape of the injection rate. However, accurate measurement of the fuel injection rate in the latter technique requires precise measurement of the bulk modulus of the working fluid as a function of the CVC pressure. The bulk modulus of commercially available diesel fuel was experimentally measured using a bespoke test rig designed and manufactured at Brunel University, which allowed bulk modulus measurements up to 600 bar. The principle of this setup was based on the application of known compressive forces upon a constant volume of fuel. A compression machine was used to apply the force to the fuel while recording the movement of the compression head. Therefore, the plot of strain versus the applied force was obtained from which the bulk modulus of the fuel was computed. The schematic drawing of the device employed for the compressibility measurements is depicted in Fig.1.

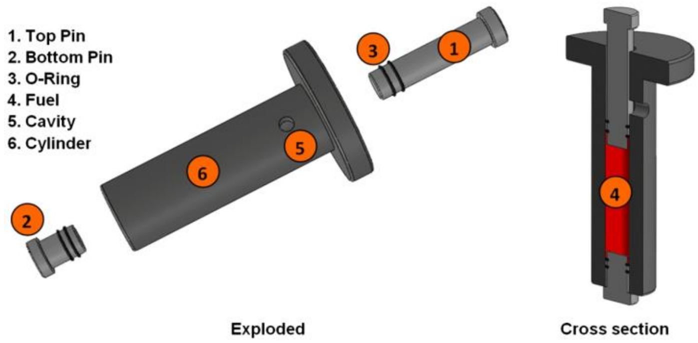

Fig.1 Schematic drawing of the bulk modulus measurement device

The bottom pin was positioned on the fixed head of the compression machine while the force was applied to the top pin through the top crosshead of the machine (i.e. the mobile crosshead). The pins were made of hardened steel to prevent buckling under high compressive loads. In order to eliminate fuel leakage from the sides of the pins, due to the pressure rise inside the cylinder, two Viton grade A o-rings were placed at the tip of both pins. The internal volume of the cylinder, made of tool steel, was dependent on the relative distance between the top and the bottom pins prior to the application of force. Hence, the bottom pin was made detachable such that the internal volume of the chamber could be easily adjusted. In order to ensure that no air was trapped inside the cylinder upon the onset of measurements, a cavity on the side of the cylinder was premeditated. Therefore, trapped air could be discharged upon the initial movement of the top pin without any force being exerted on the fuel (i.e. eliminating the compressibility effects of the trapped air inside the cylinder). The measured bulk modulus of commercially available diesel fuel as a function of pressure is shown in Fig. 2. The measurement at a given pressure reading was repeated twenty times, ensuring the repeatability of the results.

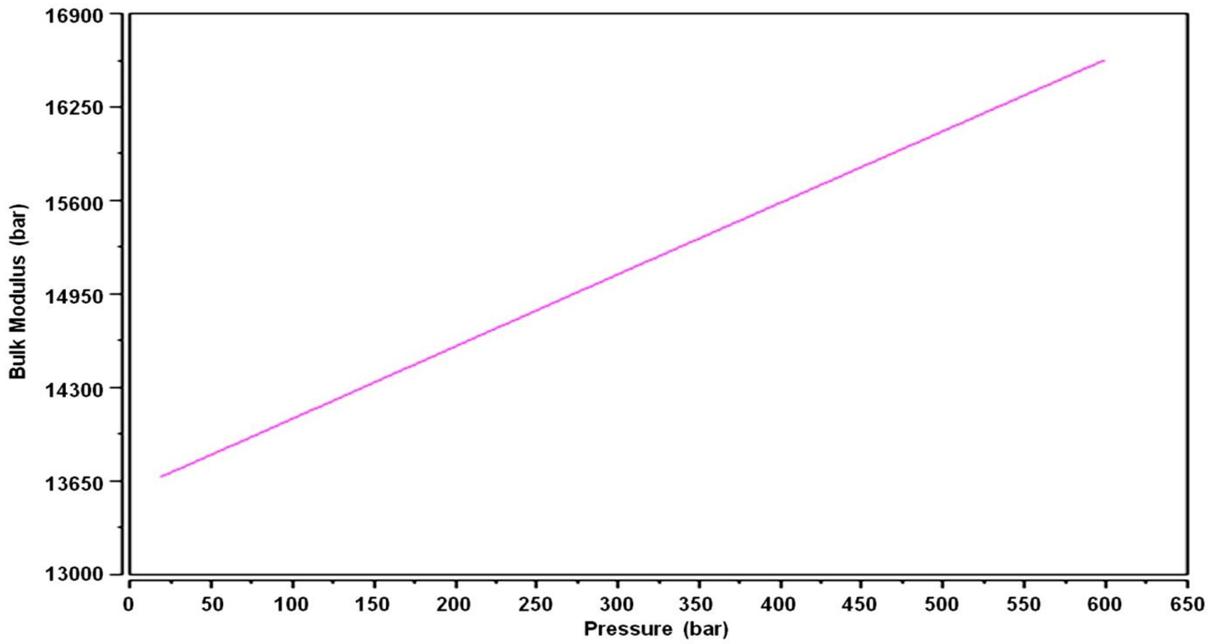

Fig. 2 Bulk modulus of standard diesel fuel

2.2 Experimental setup

A constant volume chamber, of approximately 50 cm^3, equipped with three pressure sensors was employed in this study. The first sensor, Kistler 4043A50 piezo-resistive absolute pressure transducer, measured the pressure inside the chamber prior to fuel injection (i.e. back pressure) while the second and the third sensors, Kistler 701A piezoelectric pressure transducers with high and low sensitivities, were installed for the measurement of small and large fuel quantities (i.e. pilot and main injections) respectively. A combination of a pressure relief valve and a solenoid actuator were located on top of the CVC. A schematic diagram of the experimental setup employed in this study is depicted in Fig. 3. A high pressure direct acting coaxial solenoid valve was positioned directly on top of the CVC. A Swagelok R series proportional relief valve was utilised in order to regulate the back pressure. In addition, a high precision positive displacement fuel flow meter, ONO SOKKI FP-200 series, was mounted after the pressure relief valve, measuring the quantity of the fuel injected. The fuel quantities calculated based on the application of the Zeuch's method were further validated by the fuel quantities measured by the flow meter. The fuel injector was positioned horizontally opposite the pressure sensors such that the pressure rise inside the CVC could be accurately measured.

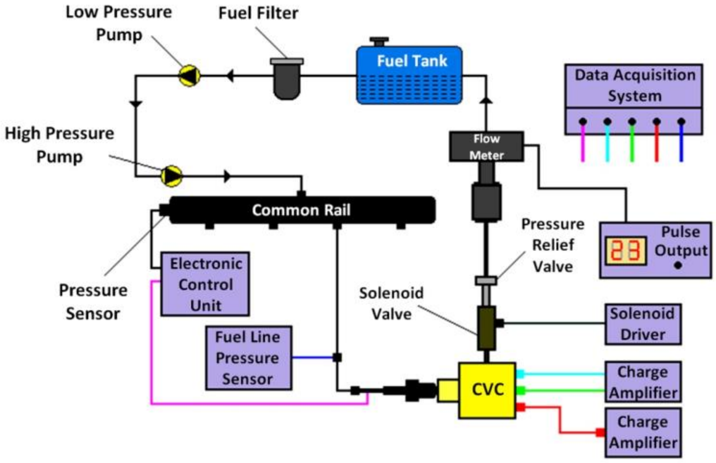

Fig. 3 Schematic diagram of fuel injection rate measurement setup

However, the accuracy of the recorded data is dependent on the relative position of the injector nozzle and the pressure transducers as well as the sensitivity of the pressure sensors. Therefore, the setup was thoroughly calibrated in order to identify the optimum distance between the injector nozzle and the pressure sensors; the optimum value in this case was identified to be 250 mm. In addition, piezoelectric pressure transducers were adopted since their accuracy is often not affected by the size or the volume of the quartz, but the geometry and the material used, enabling acquisition of accurate data even at absolute pressures ten times higher than their measuring dynamic full scale range. Furthermore, the system was leak tested prior to the onset of the fuel injection rate measurements in order to ensure that no fuel leakage occurred during the measurements.

The FIE consisted of a fuel filter, a 12V low pressure pump which drew the filtered fuel from the fuel tank, a first generation Bosch high pressure pump and a Delphi CR fuel injector. The injector utilised in this study was a Delphi multi-hole valve covered orifice (VCO) injector capable of injecting up to 1600 bar. The specifications of the FIE are listed in Table 1.

Table 1. Fuel injection equipment specifications

Injection System	
1^{st} Generation Common Rail System	
Maximum Injection Pressure	1350 bar
Delphi Standard VCO Injector	
Number of Holes	6
Hole Size	0.154 mm
Cone Angle	154^{o}
Flow Rate	0.697 l/min

2.3 Data analysis

The recorded pressure signals were filtered using fast fourier transform (FFT), equation (3), to remove the noise.

$$f_{Cutoff} = \frac{1}{n\Delta t} \tag{3}$$

Where n number of data points considered in every filtering region

Δt time interval between two adjacent data points

Therefore, larger values of n result in lower cut-off frequencies, hence greater degree of smoothing. The cut-off frequency of 5 kHz was used in this study. The subsequent calculations and analysis were performed using the filtered pressure signals.

3 ENGINE AND MEASUREMENT TECHNIQUES

All experimental testing in this study was carried out in a single cylinder high-speed optical engine equipped with a production cylinder head, designed to be representative of a typical modern high-speed direct injection (HSDI) diesel engine. The engine specifications are depicted in Table 2. The engine consisted of a Ricardo Hydra engine crankcase, extended cylinder block and piston, and a standard production Ford 2.0 litre ZSD 420 Duratorq engine cylinder head. The details of the common rail fuel injection system are given in Table 1.

Table 2. Single cylinder optical engine specifications

Ricardo Hydra Single-Cylinder Engine	
Bore	86 mm
Stroke	86 mm
Swept Volume	499 cm^3
Compression Ratio	16:1
Piston Bowl	43.4/11.6 mm
	Re-entrant bowl with flat bottom
Swirl Ratio (Ricardo)	1.4

In this study, a Kistler 6125 piezoelectric pressure transducer was installed in place of the glow plug for in-cylinder pressure measurement and heat release analysis. Optical access was provided by the Bowditch piston design which allowed for the visualisation of the combustion chamber through the axis of the cylinder via a glass window, made from fused silica, mounted in the crown of the piston. An extended piston and cylinder block were required in order to accommodate such an optical configuration which consisted of lower and upper parts with a 45° angled mirror, made of glass with aluminised front surface, between the sections. Therefore, the combustion chamber and cylinder walls could be fully visualised through such an optical setup, Fig. 4.

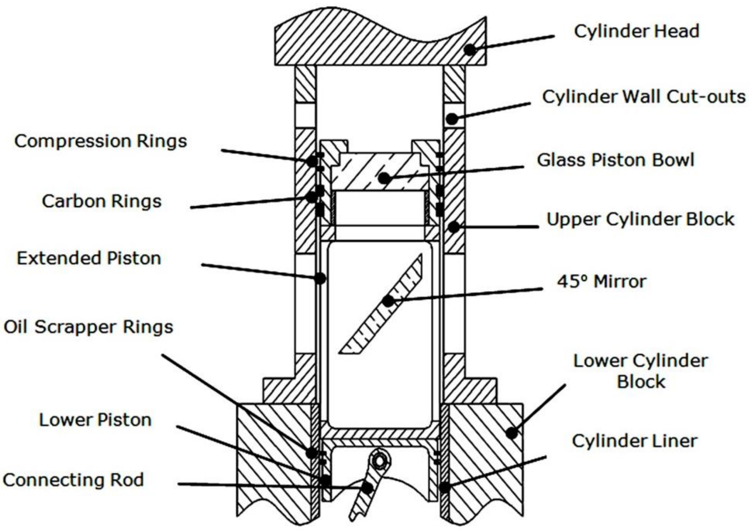

Fig. 4 Sectional schematic view of the optical layout

In addition, the upper cylinder block had three rectangular wall cut-outs which can be fitted with glass windows, made of fused silica, for side optical access. Two of these windows were in the same plane allowing laser sheet imaging, Fig. 4, while the third window was positioned at 90°, premeditated for imaging and detection purposes.

3.1 Conventional measurements

For the injection strategies studied, in-cylinder pressure data from 20 consecutive engine cycles was recorded from which the ensemble-averaged net heat release rate (HRR) was calculated through the application of the first law of thermodynamics [**54**], equation (4).

$$HRR = \frac{\gamma}{\gamma - 1} p \frac{dV}{dt} + \frac{1}{\gamma - 1} V \frac{dp}{dt} \qquad (4)$$

In addition, the soot and gaseous exhaust emissions were measured to assess the effect of two-stage fuel injection and dwell angle on engine performance and emissions. The gaseous exhaust emissions of CO, CO_2, O_2, uHC and NOx were measured by means of a Horiba MEXA-7170DEGR analyser system while the soot emission was measured using an AVL 415 smoke meter.

3.2 High speed spray and combustion visualisation

High speed video imaging was employed to record colour images of fuel sprays during the injection period and subsequent combustion process, Fig. 5. A NAC Memrecam FX6000 high speed colour video camera was used which was equipped with a high speed complementary metal–oxide semiconductor (CMOS) sensor. The high speed camera was synchronised to the pulsed laser outputs to capture videos at 10,000 frames per second with an image resolution of 512 x 248 pixels. A Nikon 50mm f.1.4 lens was used. A LED installed in the field of view of the camera provided the reference signal at top dead centre (TDC) in the high speed video images. It is important to note that although the first frame with visible fuel spray is referred to as the start of injection, the actual start of injection in some of the presented frames may not correspond to this point due to inter frame rate of the high speed camera utilised.

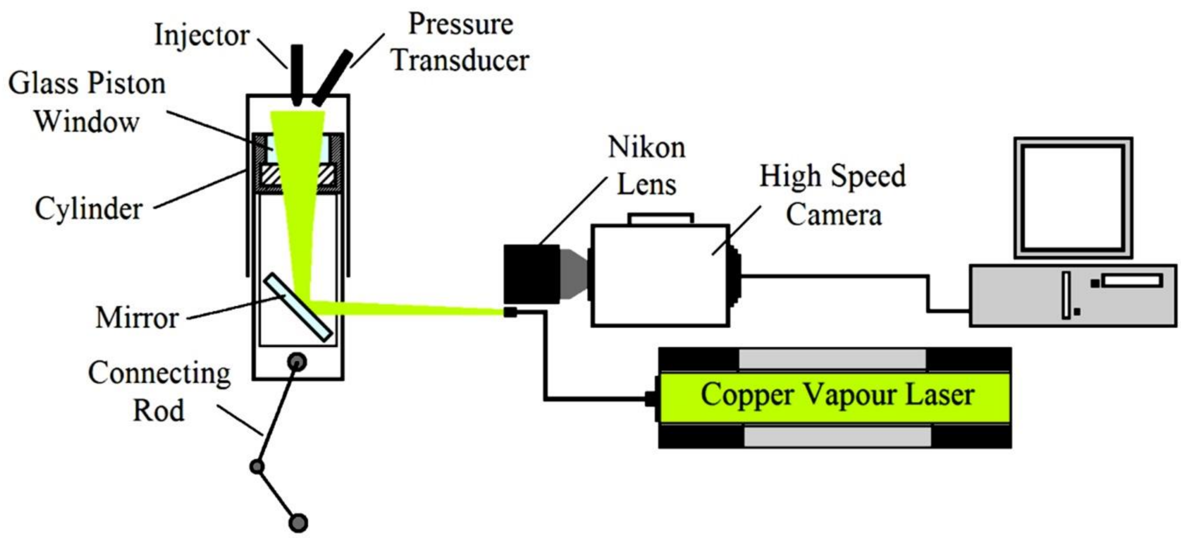

Fig. 5 Schematic diagram of direct combustion visualisation setup

The observation field through the piston window is illustrated in Fig. 6. In order to visualise the fuel sprays, a high repetition copper vapour Laser was utilised. The output of the laser was delivered to the engine via an optical fibre so that the whole combustion chamber could be illuminated by the divergent laser beam leaving the optical fibre. The short laser pulse of 30ns effectively defined the exposure time of the spray image, which was critical to obtain sharp images of sprays travelling at very high speed.

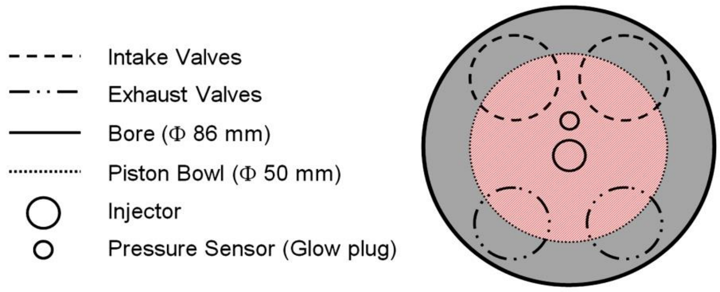

Fig. 6 Observation field through piston window

4 ENGINE OPERATING CONDITIONS

The mechanical and thermal stresses the optical components are exposed to during firing cycles are substantial, thus the operating time of optical engines is limited. As a result, both the coolant and the lubricating oil were heated prior to the experiment to ensure reasonable engine temperature was achieved. In this study injection pulse widths were set to produce 30%/70%, 50%/50% and 70%/30% two-stage fuel injection strategies with variable dwell angle under part load operating conditions at the engine speed of 1500 rpm, Table 3.

Table 3. Test conditions

Intake Air	100°C Naturally Aspirated (NA), Without EGR
Engine Speed	1500 rpm
Fuel	Commercially Available 49.1 CN Diesel
Fuelling Demand	20 mm^3/cycle
Load	≈ 72% of NA Full Load, 27.7:1 AFR
Injection	1200 bar
Piston Bowl	Glass – Pressure, Optical Techniques Metal – Soot, Emissions

The two-stage fuel Injection strategies were selected such that the injection timing of the second injection remained constant at TDC while the injection timing of the first injection was varied. A typical profile of the current that energises the solenoid of the electronically controlled fuel injector is illustrated in Fig. 7.

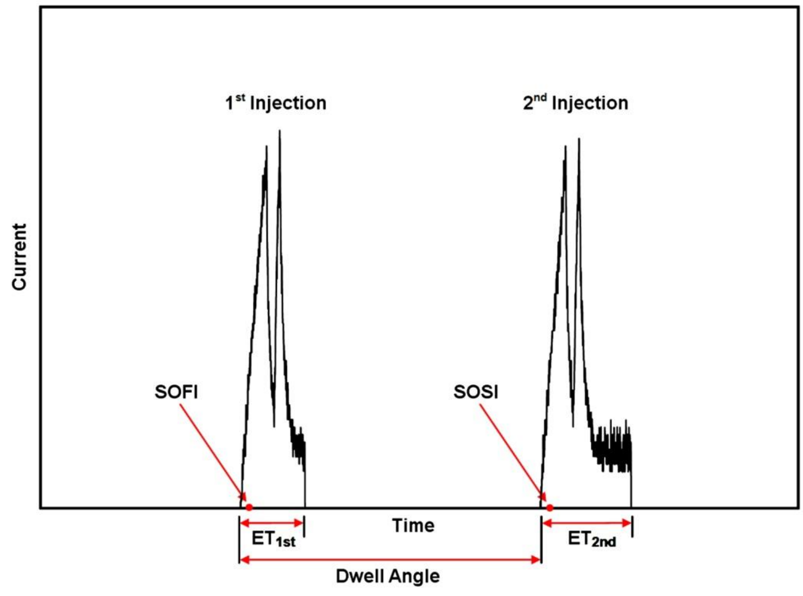

Fig. 7 Schematic representation of injector current waveform

The current waveform supplied to the injector can be characterised by the following definitions,

- SOFI: Start of the first injection
- ET_{1st}: Energising time of the first injection
- SOSI: Start of the second injection
- ET_{2nd}: Energising time of the second injection
- Dwell angle (DA): The time interval between the start of the first injection and the start of the second injection

It is important to note that there exists a time lag between the start of the injector current waveform and the start of fuel injection due to the inertia of the system as illustrated in Fig. 7. In order to allow comparative analysis of the results, single injection strategies were also performed, serving as the baseline. The tested strategies are detailed in Table 4.

Table 4. Injection strategies

Strategy	Test No	SOI (CAD ATDC)		ET (μs)		DA (CAD)
Single Injection	**A1**	-15		596		N/A
	A2	-10		596		
	A3	-5		596		
	A4	TDC		596		
		1st	**2nd**	**ET_{1st}**	**ET_{2nd}**	
Two-stage 30%/70%	**B1**	-20	TDC	345	487	20
	B2	-15	TDC	345	487	15
	B3	-10	TDC	345	487	10
	B4	-5	TDC	345	487	5
Two-stage 50%/50%	**D1**	-20	TDC	422	422	20
	D2	-15	TDC	422	422	15
	D3	-10	TDC	422	422	10
	D4	-5	TDC	422	422	5
Two-stage 70%/30%	**F1**	-20	TDC	487	345	20
	F2	-15	TDC	487	345	15
	F3	-10	TDC	487	345	10
	F4	-5	TDC	487	345	5

5 RESULTS AND DISCUSSION

5.1 Effect of two-stage fuel injection and dwell angle on fuel injection quantity

The measured injection rate profiles for the tested two-stage fuel injection strategies are presented in Fig. 8.

In the case of 30%/70% injections (B1 to B4), although the injection duration of the first fuel injection event was identical for 10 (B1), 15 (B2) and 20 (B3) crank angle degree (CAD) dwell angles, the quantity of fuel injected fluctuated by approximately 10%, Table 5. This was mainly attributed to the design limitations of the injector utilised as well as the transient nature of the fuel flow under such short opening and closing of the injector. However, the quantity of fuel injected during the first injection remained almost identical for 50%/50% (D1 to D4) and 70%/30% (F1 to F4) strategies due to relatively longer injection duration. In contrast, the quantity of fuel during the second injection was found to be dependent on the dwell angle utilised as shown in Fig. 8 and Table 5. These considerable variations in the total injected fuel quantity were mainly attributed to the design limitations of the injector utilised as well as the adverse effects of pressure waves in the high pressure fuel line, caused by the first injection.

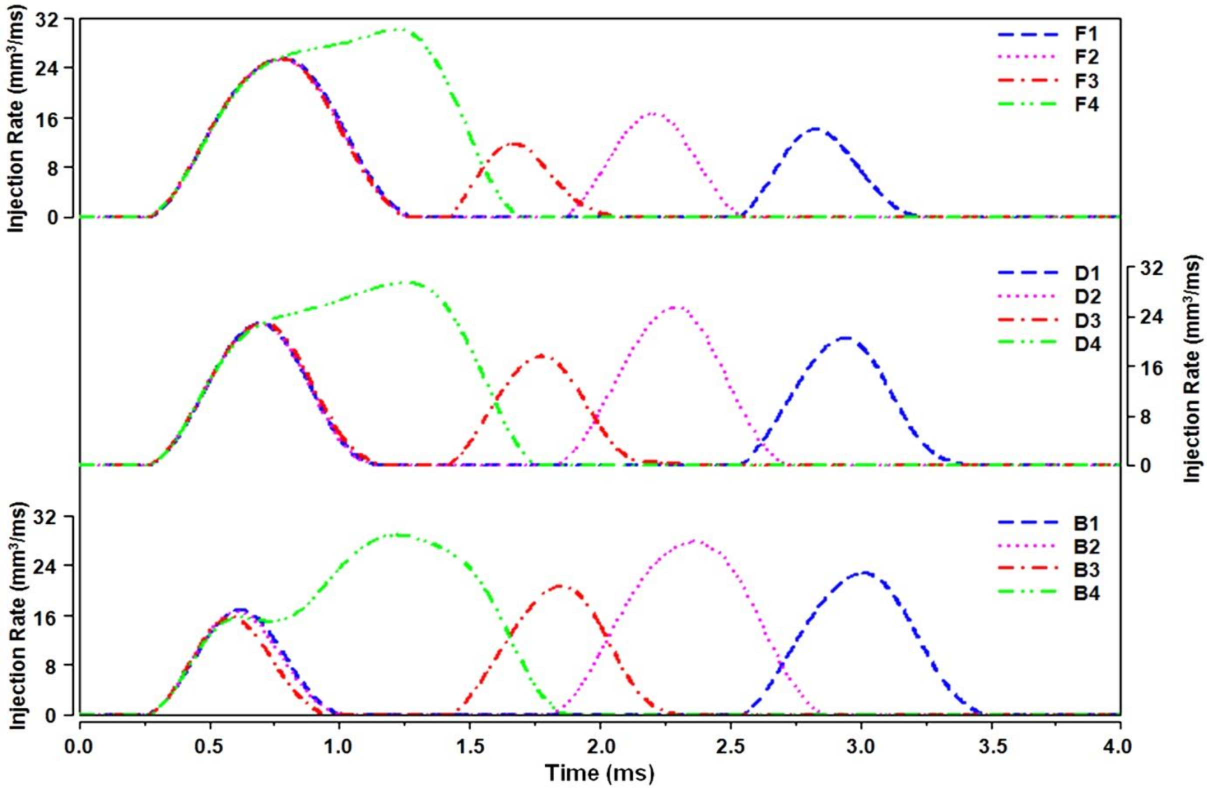

Fig. 8 Injection rate profiles for two-stage injection strategies

Table 5. Fuel injection quantity

Test Number	Injection Pressure (bar)	1st Fuel Injection Quantity (mm^3)		2nd Fuel Injection Quantity (mm^3)		Total Fuel Injection Quantity (mm^3)		Total Fuel Quantity Percentage Error (%)
		Desired	Actual	Desired	Actual	Desired	Actual	
B1	1200	6.0	6.3	14.0	11.0	20.0	17.3	-13.5
B2	1200	6.0	6.0	14.0	15.9	20.0	21.9	+9.5
B3	1200	6.0	5.4	14.0	8.9	20.0	14.3	-28.5
B4	1200	6.0	26.9	14.0	26.9	20.0	26.9	+34.5
D1	1200	10.0	10.0	10.0	8.7	20.0	18.7	-6.5
D2	1200	10.0	10.0	10.0	11.6	20.0	21.6	+8.0
D3	1200	10.0	10.0	10.0	7.3	20.0	17.3	-13.5
D4	1200	10.0	28.0	10.0	28.3	20.0	28.3	+41.5
F1	1200	14.0	14.0	6.0	4.9	20.0	18.9	-5.5
F2	1200	14.0	14.0	6.0	6.0	20.0	20.0	0.0
F3	1200	14.0	14.0	6.0	3.7	20.0	17.7	-11.5
F4	1200	14.0	27.3	6.0	27.3	20.0	27.3	+36.5

The fuel line pressure traces for the studied two-stage strategies are presented in Fig. 9. The same pattern in fuel line pressure fluctuations was observed for all the studied cases, this was mainly due to identical hydraulic properties of the tested fuel. The first pressure drop was due to the first fuel injection event. However, the subsequent pressure fluctuations were due to the sudden closure of the injector valve, creating so-called "water hammer" in the high pressure fuel line. Water hammer is created when a valve is suddenly closed in a pipe, the resultant pressure wave travels in the pipe periodically. This oscillation is eventually dampened due to viscous effects. The results suggested that the quantity of the injected fuel was dependent on the magnitude and frequency of the pressure wave in the fuel line. In the case of 10 CAD dwell angle, the second fuel injection took place when the fuel line pressure was rapidly descending (i.e. pressure wave travelling towards the rail) which resulted in the lowest fuel injection quantity. The same explanation holds true for 20 CAD dwell angle. However, in this case the effect of pressure fluctuation was less paramount since the longer dwell angle used led to considerable damping of the pressure waves. In contrast, the second fuel injection in the case of 15 CAD dwell angle took place when the fuel line pressure was rapidly increasing (i.e. pressure wave travelling towards the injector) which resulted in higher injected fuel quantity. In production engines, it is necessary to compensate for such variations in the injected fuel quantity by either careful characterisation of the fuel injection system or modifying the shape and/or length of the high pressure lines. The result for 5 CAD dwell angle indicated that this dwell angle was not sufficient for the injector to fully close prior to the onset of the second injection, thus almost replicating an extended single injection. This resulted in the total injected fuel quantities substantially higher than the desired quantity of 20 mm^3, Table 5. The effects of such inconsistency in fuel delivery on the combustion and emissions characteristics were then investigated.

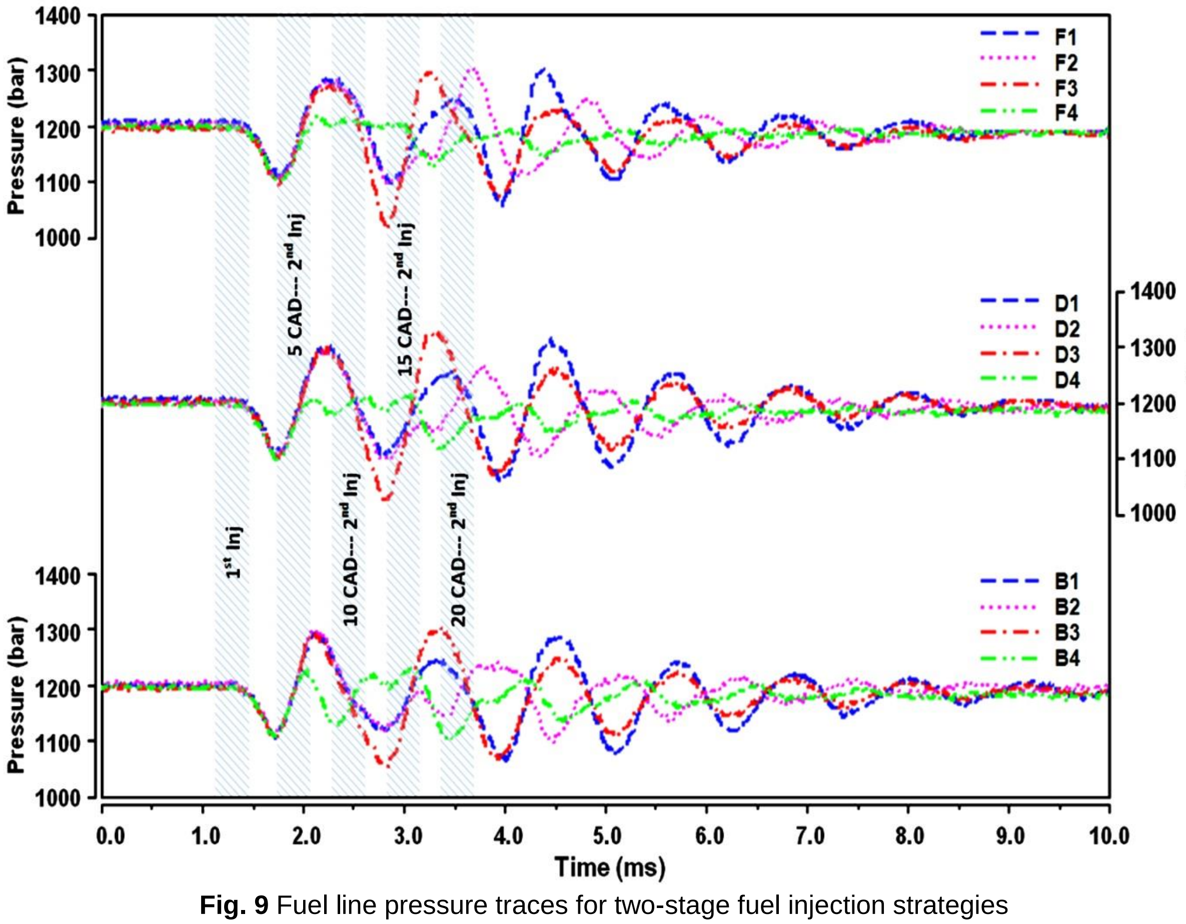

Fig. 9 Fuel line pressure traces for two-stage fuel injection strategies

5.2 Effect of two-stage fuel injection and dwell angle on combustion and emissions

The calculated and measured data for the injection and combustion characteristics are listed in Table 6. The Injection duration for each injection strategy was determined based on the injection rate profiles obtained through the Zeuch's method while the IMEP values and the start of combustion timings were calculated from the in-cylinder pressure and heat release rate data respectively. The Ignition delay was also determined from the heat release rate data as the time between the start of the first injection and the onset of the main heat release rate.

Table 6. Injection and combustion characteristics

Test Number	Injection Pressure (bar)	Total Injection Duration (CAD)	IMEP (bar)	Start of Combustion (CAD ATDC)	Ignition Delay (CAD)
A1	1200	5.4	3.06	-6.6	8.4
A2	1200	5.4	3.17	-2.6	7.4
A3	1200	5.4	3.46	2.6	7.6
A4	1200	5.4	4.43	12.6	12.6
B1	1200	7.6	3.56	-12.2	7.8
B2	1200	7.6	4.28	-8.8	6.2
B3	1200	7.6	2.86	-5.8	4.2
B4	1200	7.6	5.42	2.6	7.6
D1	1200	7.6	2.65	-12.2	7.8
D2	1200	7.6	4.24	-8.6	6.4
D3	1200	7.6	1.98	-5.2	4.8
D4	1200	7.6	5.43	2.2	7.2
F1	1200	7.6	1.54	-11.2	8.8
F2	1200	7.6	3.71	-7.4	7.6
F3	1200	7.6	2.62	-4.4	5.6
F4	1200	7.6	5.74	3.4	8.4

The in-cylinder pressure and heat release rate data for the single injection strategies are depicted in Fig. 10. The peak in-cylinder pressure decreased as the injection timing was retarded. This was mainly attributed to late initiation of the combustion process during the expansion stroke where the piston was descending after TDC due to retarded fuel injection timing.

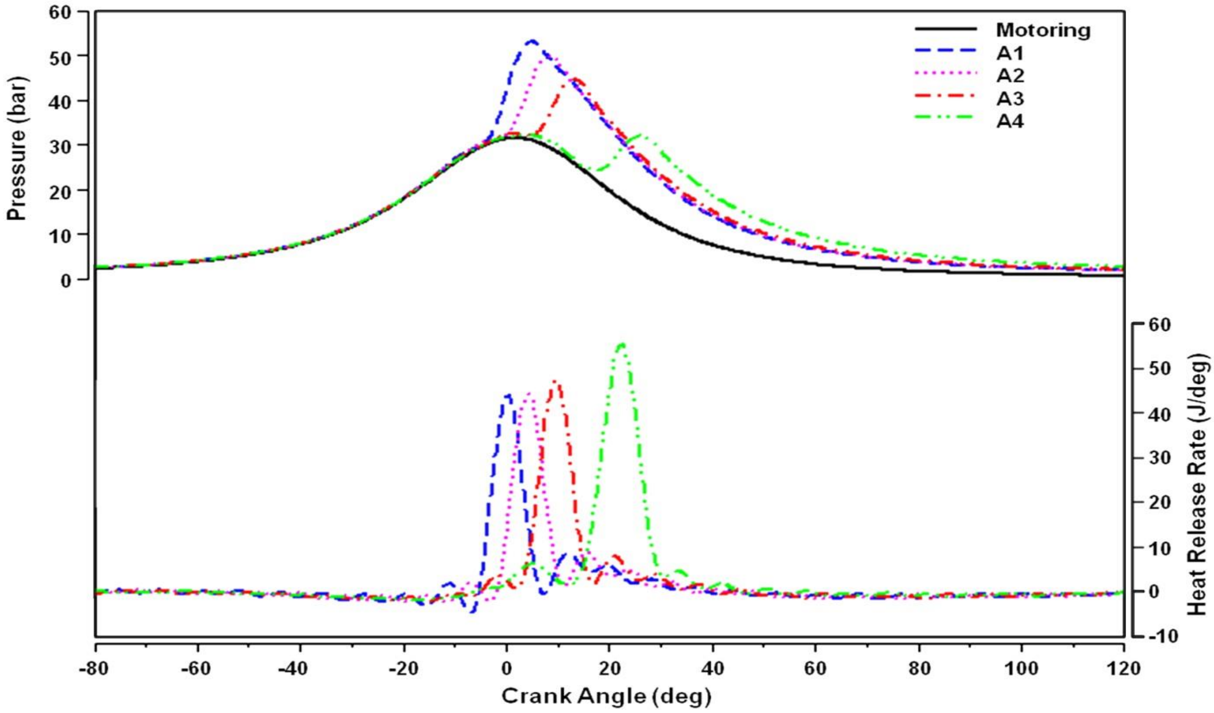

Fig. 10 In-cylinder pressure and heat release rate for single injection strategies

The heat release rate curves exhibited a drop due to charge cooling effect shortly after the onset of the first fuel injection. Subsequently, the rate of heat release rapidly increased due to the premixed combustion. As given in Table 6, the ignition delay period decreased and the percentage of premixed combustion became less as the injection timing was retarded towards TDC. The reduction in the amount of heat released from the fast premixed combustion with late injection is compensated for by the faster heat release of combustion in a smaller volume near TDC. As a result, the peak heat release rate remained almost constant for A1, A2 and A3 strategies. However, this trend was not observed for A4 strategy. In this case the ignition delay was much longer and more heat release took place due to premixed combustion, resulting in greater heat release rate. This was mainly due to initiation of combustion during the expansion stroke when the in-cylinder pressure and temperature were reduced. Though, the peak in-cylinder pressure was lower as the combustion occurred in a larger cylinder volume.

The in-cylinder pressure and heat release rate data for the two-stage injection strategies are depicted in Fig. 11 and Fig. 12 respectively.

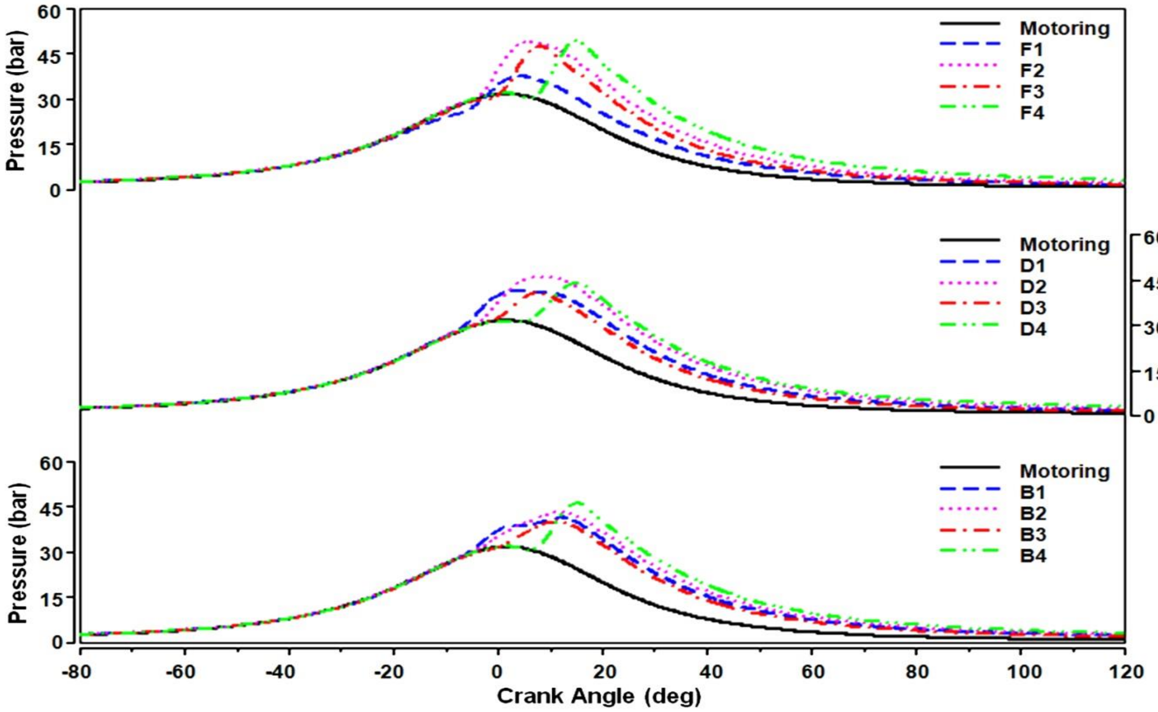

Fig. 11 In-cylinder pressure for two-stage injection strategies

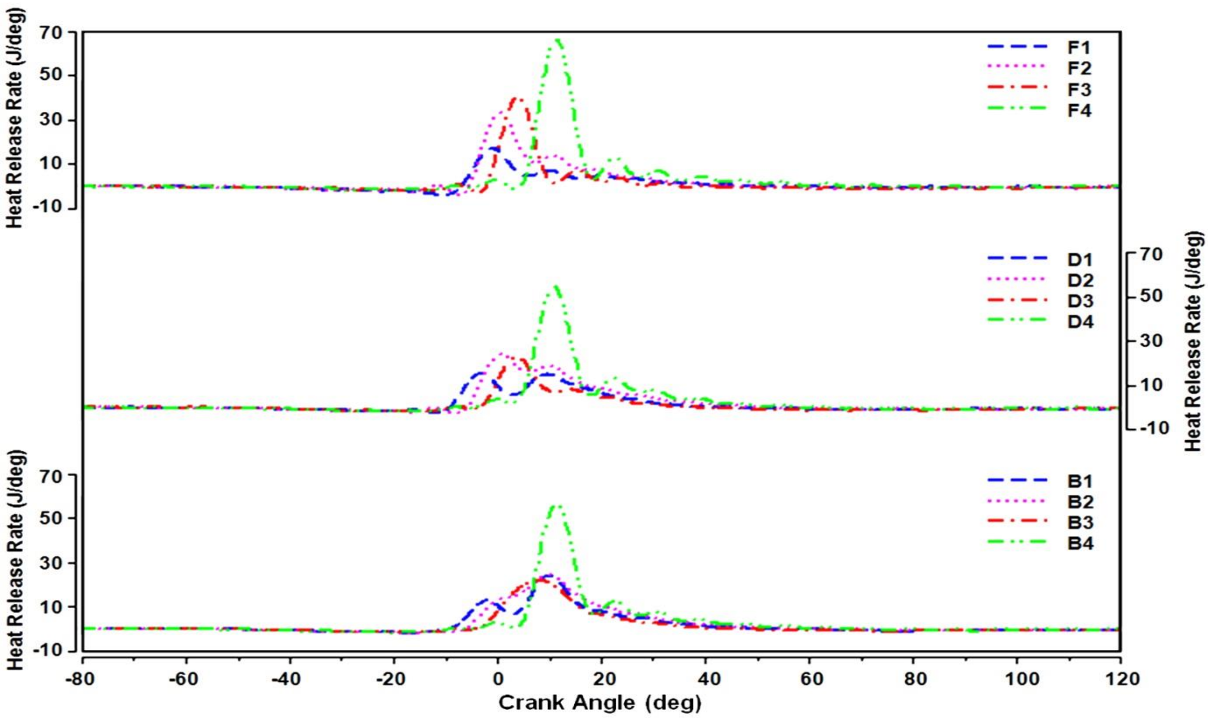

Fig. 12 In-cylinder heat release rate for two-stage injection strategies

As shown in these figures, when the two-stage injection was employed, in-cylinder pressure and heat release rate curves exhibited different trends from those of single injections. The peak in-cylinder pressure first increased as the first injection was retarded from 20 to 15 CAD BTDC and then dropped slightly in the cases of 10 CAD dwell angle. The corresponding heat release curves showed that the heat release rate increased as the first injection timing was retarded, instead of remaining constant as with the single injections. The 5 CAD dwell angle resulted in the highest peak in-cylinder pressure and heat release rate due to mainly the larger amount of fuel injected as the injector failed to close prior to the onset of the second injection, Fig. 8. Therefore, the strategies with such a dwell angle will not be discussed further.

The heat release rate curves in Fig. 11 exhibited a drop due to charge cooling effect shortly after the onset of the first fuel injection. Subsequently, the rate of heat release rapidly increased due to the premixed combustion. As shown in Table 6, the ignition delay period decreased, due to improved fuel evaporation and mixing effects closer to TDC, as the injection timing was retarded. However, unlike the single injection strategies the percentage of combustion during the peak heat release period increased with shorter ignition delay. In order to determine the primary causes of such a trend, high speed fuel spray and combustion visualisation technique was applied, Fig. 13, in which the start of the first injection (SOFI), first visible combustion (FVC), start of the second injection (SOSI) and the maximum heat release rate (MHRR) for D1, D2 and D3 strategies were studied and compared.

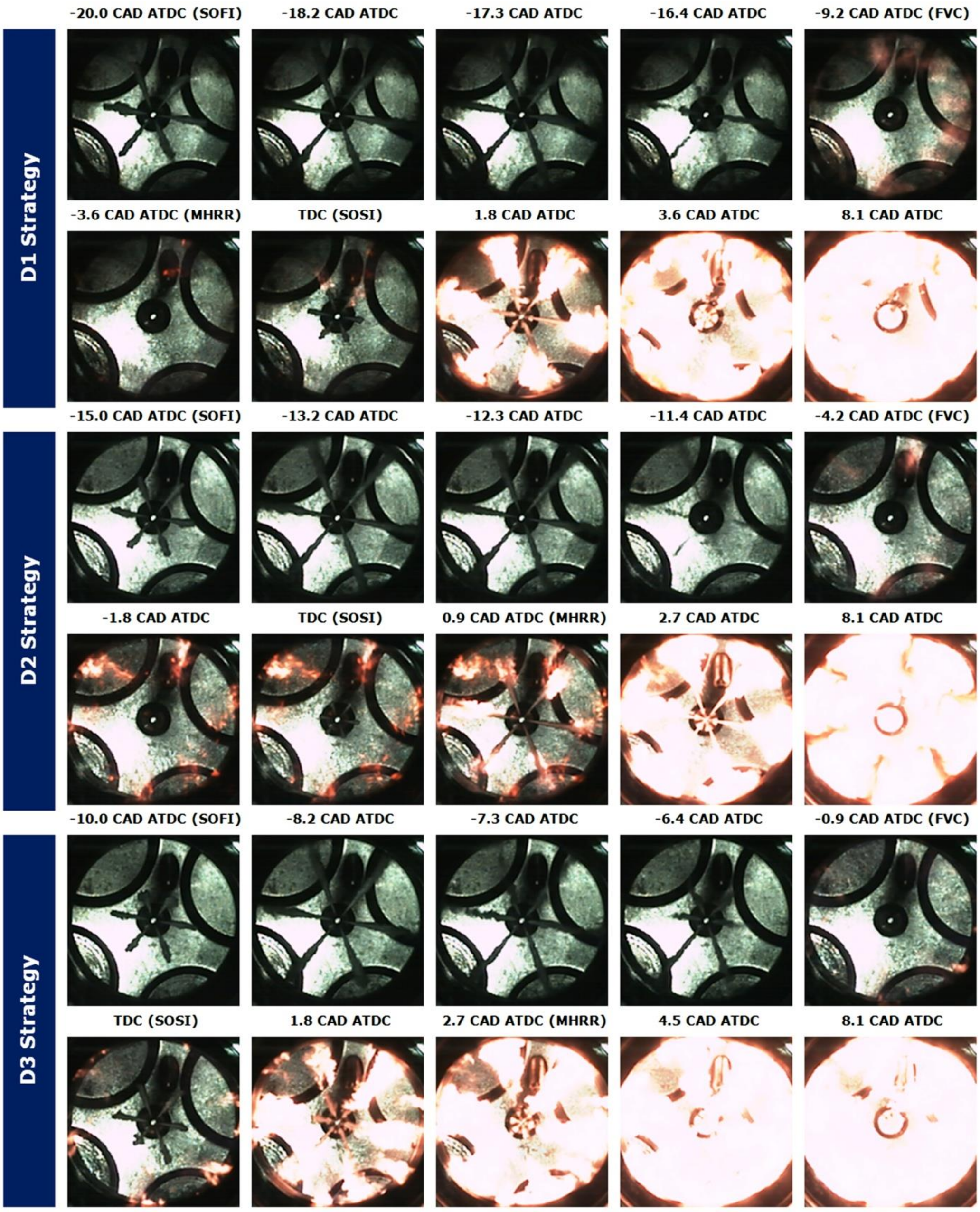

Fig. 13 Combustion image sequence for 50%/50% injection strategies

The asymmetry of the fuel sprays during the initial stages of fuel injection is evident in Fig. 13. At low needle lift condition the VCO nozzles suffer from uneven distribution of pressure field inside the nozzle holes due to eccentric or radial motion of the needle tip, caused by the close proximity of the needle seat to the nozzle holes. The high speed images obtained revealed that the increase in the percentage of combustion near and shortly after TDC during the peak heat release rate period was due to the interaction between the first and the second injections, whereby the fuel sprays during the second injection at TDC were injected into burning regions generated by the combustion of premixed fuel and air during the first injection. As a result, the premixed combustion of fuel from the first injection was intensified by the participation of the second injection. The effect of such an interaction became more pronounced as the first injection timing was moved closer to TDC, where higher percentage of premixed combustion took place prior to the onset of the second fuel injection. The same trend was observed for 30%/70% and 70%/30% injection strategies. From the results obtained, it is evident that the design limitations of the FIE as well as the possibility of interactions between the fuel injections during the combustion are amongst the complications that may be encountered in the application of two-stage or multiple injection strategies. Therefore, thorough characterisation of the FIE and careful selection of injection strategies are essential for satisfactory implementation of such advanced injection modes.

The in-cylinder pressure derivative for the studied single and two-stage injection strategies is presented in Fig. 14. It is clearly evident that the quantity of the first injection had a significant effect on the rate of in-cylinder pressure rise, progressively increasing as the quantity of the first injection was increased, though it remained lower than those of single injection strategies. The in-cylinder pressure derivative is an indication of the combustion noise and the mechanical stresses the engine parts are exposed to. Therefore, the results suggest that the combustion noise and also the mechanical stresses the engine parts are exposed to can be notably decreased with two-stage fuel injection. However, these aspects depend on the fuel injection strategy and the engine speed, thus thorough assessment of such a phenomenon under various engine operating conditions is required in order to draw an explicit conclusion.

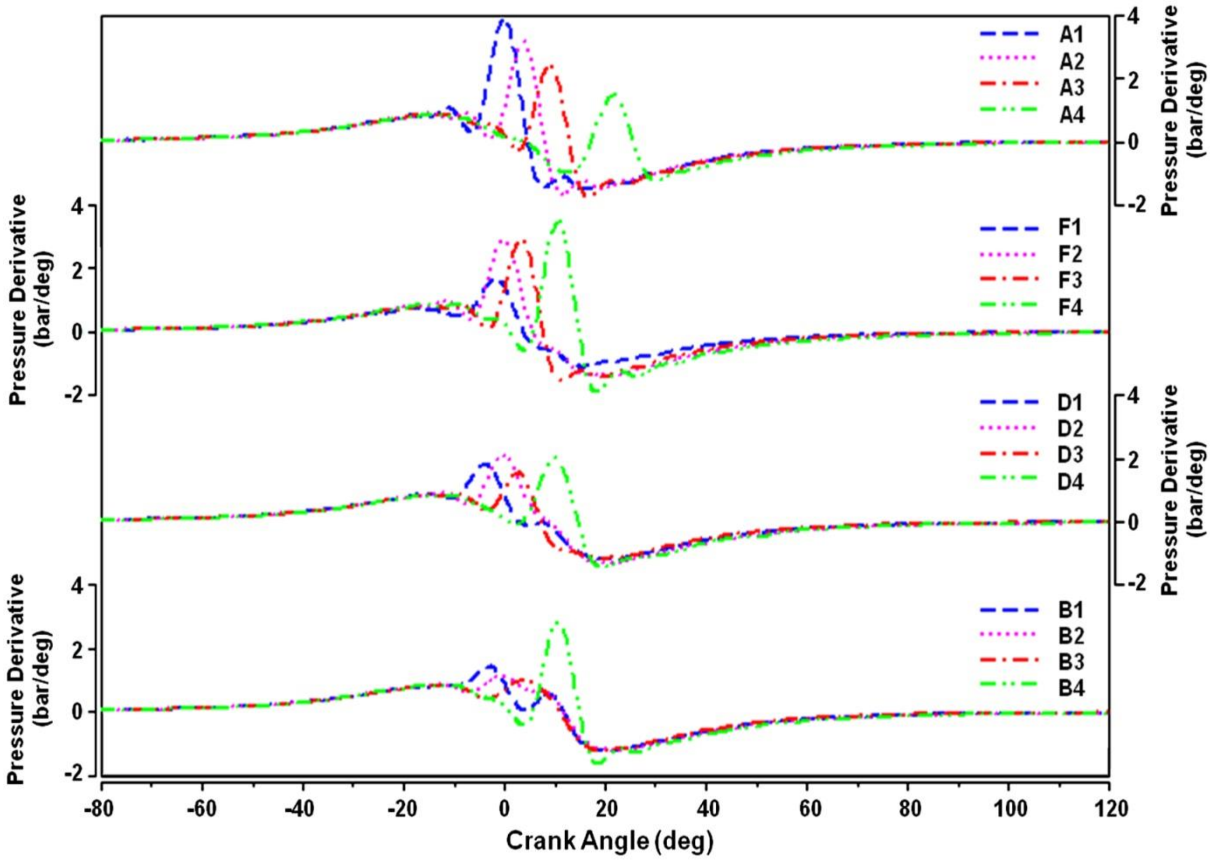

Fig. 14 In-cylinder pressure derivative for single and two-stage injection strategies

The soot, NOx and uHC emissions results are depicted in Fig. 15. The substantial variations in the engine output and exhaust emissions for the investigated two-stage injection strategies were primarily caused by the inconsistency in the total fuel quantity injected, due to the effect of tow-stage injection and the dwell angle, as well as the interaction between the first and the second injections. Nevertheless, B2, D2, F2, A3 and A4 strategies can be compared since the total injected fuel quantities were identical and the IMEP values were comparable.

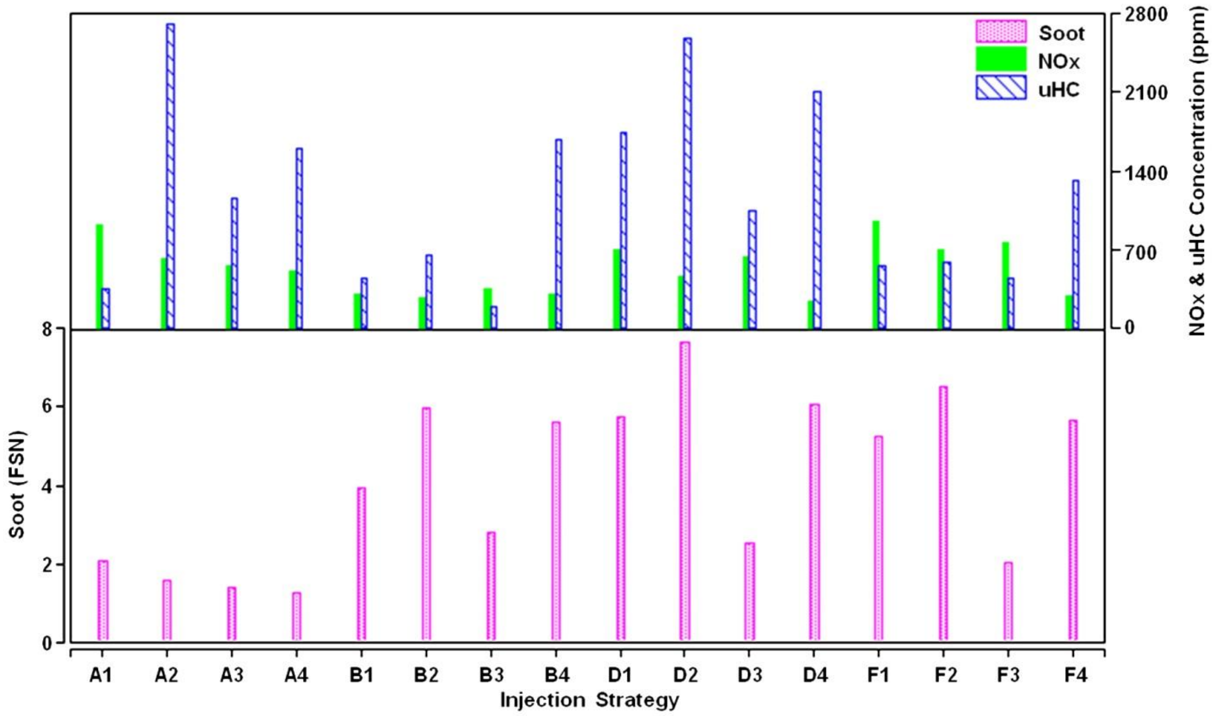

Fig. 15 Exhaust emissions for single and two-stage injection strategies

In the case of two-stage injection, the percentage of fuel injected during the first injection was found to correlate with the engine emissions. As more fuel was injected in the first injection, NOx and soot emissions increased while uHC emission decreased. The results also suggest that two-stage injection appears to affect the NOx-soot trade-off. As the quantity of fuel during the first injection was reduced from 70% to 30%, NOx, soot and uHC emissions were simultaneously reduced due to improved mixing and air utilisation. Although lower NOx emission was obtained in comparison to single injection strategies, soot emission was higher. This was mainly attributed to the interaction between two consecutive fuel injection events, whereby the fuel sprays during the second injection were injected into burning regions, as previously illustrated in Fig. 13. Moreover, the selected dwell angles in this study led to the continuation of combustion into the expansion stroke, curtailing soot oxidation. The results suggest that an optimum fuel quantity in the first injection exists, 0-30%, with which simultaneous reduction of NOx, soot and uHC emissions can be achieved with the added benefits of improved engine performance, fuel economy and combustion noise. In this case, most of the fuel injected during the first injection is consumed in the premixed burn while the remnant of the fuel injected during the second injection sustains the diffusion burn provided that suitable dwell angle is utilised, eliminating interactions between the two fuel injections.

6 CONCLUSIONS

In this paper, the hydraulic effects of two-stage injection on the fuel injection system performance and in-cylinder mixture formation, combustion and emissions were investigated in a single cylinder CR fuel injection optical diesel engine. The fuel injection rate and interaction between two consecutive fuel injection events were quantified using a fuel injection characterisation rig. The in-cylinder process was studied by means of detailed heat release analysis and high speed fuel spray and combustion visualisation technique. The main findings can be summarised as follows: regarding the studied two-stage injection strategies with variable dwell angle at 1200 bar injection pressure and the engine speed of 1500 rpm.

- Significant interactions were found between two closely spaced two-stage injections in a solenoid CR fuel injector, mainly due to the limitations of the injector utilised and the presence of pressure waves in the fuel lines. Therefore, care must be taken to ensure that such effects are considered and accounted for in advanced diesel combustion modes which require multiple injections.

- The in-cylinder high speed spray imaging and combustion visualisation technique provided direct evidence of the interaction between combustion and fuel injection. The direct fuel injection into the premixed combustion from the first injection led to more pronounced heat release rate seen amongst the studied strategies.

- The results from the single and two-stage injection strategies with similar total injected fuel quantities and IMEP values were compared, indicating the possibility of simultaneous reduction of NOx, soot and uHC emissions. The results suggested that an optimum fuel quantity in the first injection exists, 0-30%, with which simultaneous reduction of NOx, soot and uHC emissions can be achieved with the added benefits of improved engine performance, fuel economy and combustion noise. However, the tested two-stage injection strategies resulted in higher soot emissions, mainly due to the interaction between two consecutive fuel injection events, whereby the fuel sprays during the second injection were injected into burning regions as well as reduced soot oxidation.

Although the engine operating conditions and the injection parameters investigated in this study were different to those previously studied, the findings are in good agreement with the results previously reported by other research groups [**30**, **34-36**, **43**, **44**]. Nevertheless, in order to identify the true effects of two-stage injection with variable dwell angle on diesel combustion and emissions further detailed characterisation of the fuel injection system is required. In addition, an explicit conclusion on the advantages of two-stage fuel injection in comparison to that of conventional single injection can only be drawn provided that the effects of such an injection mode under various engine operating conditions are thoroughly assessed.

ACKNOWLEGMENTS

The financial and technical support provided by Delphi Diesel Systems is gratefully acknowledged.

REFERENCES

1. European Automobile Manufacturers' Association, http://www.acea.be, (accessed 15 March 2010).
2. **Pierpont, D. A., Montgomery, D. T.,** and **Reitz, R.D.** Reducing Particle and NOx Using Multiple Injection and EGR in a D.I. Diesel. SAE paper 950217, 1995.
3. **Nehmer, D. A.** and **Reitz, R. D.** Measurement of the Effect of Injection Rate and Split Injections on Diesel Engine Soot and NOx Emissions. SAE paper 940668, 1994.
4. **Tow, T. C., Pierpont, D. A.,** and **Reitz R. D.** Reducing Particulate and NOx Emissions by Using Multiple Injections in a Heavy Duty D.I. Diesel Engine. SAE paper 940897, 1994.
5. **Zambare, V. V.** and **Winterbone, D. E.** Photographic Investigation of Multi-Stage Fuel Injection in Single Cylinder DI Diesel Engine. SAE paper 1999-01-1501, 1999.
6. **Juneja, H., Ra, Y.,** and **Reitz, R. D.** Optimization of Injection Rate Shape Using Active Control of Fuel Injection. SAE paper 2004-01-0530, 2004
7. **Tanabe, K., Kohketsu, S.,** and **Nakayama, S.** Effect of Fuel Injection Rate Control on Reduction of Emissions and Fuel Consumption in a Heavy Duty DI Diesel Engine. SAE paper 2005-01-0907, 2005.
8. **Yun, H.** and **Reitz, R. D.** Combustion Optimization in the Low-Temperature Diesel Combustion Regime. *Int. J. Engine Res.*, 2005, **6**, 513-524.
9. **Alriksson, M.** and **Denbratt, I.** Low Temperature Combustion in a Heavy Duty Diesel Engine Using High Levels of EGR. SAE paper 2006-01-0075, 2006.
10. **Dec, J. E.** Advanced Compression-Ignition Engines-Understanding the In-Cylinder Processes. *Proc. Combust. Inst.*, 2009, **32**, 2727-2742.
11. **Li, T., Suzuki, M.,** and **Ogawa, H.** Effect of Two-Stage Injection on Unburned Hydrocarbon and Carbon Monoxide Emissions in Smokeless Low-Temperature Diesel Combustion with Ultra-High Exhaust Gas Recirculation. *Int. J. Engine Res.*, 2010, **11**, 345-354.

12. **Anselmi, P., Kashdan, J., Bression, G., Ferrero-Lesur, E., Thirouard, B.** and **Walter, B.** Improving Emissions, Noise and Fuel Economy Trade-Off by using Multiple Injection Strategies in Diesel Low Temperature Combustion (LTC) Mode. SAE paper 2010-01-2162, 2010.
13. **Knight, B. M., Bittle, J. A.,** and **Jacobs, T. J.** Characterizing the Influence of EGR and Fuel Pressure on the Emissions in Low Temperature Diesel Combustion. SAE paper 2011-01-1354, 2011.
14. **Lu, X., Han, D.,** and **Huang, Z.** Fuel Design and Management for the Control of Advanced Compression-Ignition Combustion Modes. *Prog. Energy Combust. Sci.*, 2011, **37**, 741-783.
15. **Aceves, S. M., Flowers, D. L., Martinez-Frias, J., Smith, J. R., Dibble, R., Au, M.,** and **Girard, J.** HCCI Combustion: Analysis and Experiments. SAE paper 2001-01-2077, 2001.
16. **Milovanovic, N., Chen, R., Dowden, R.,** and **Turner, J.** An Investigation of Using Various Diesel-Type Fuels in Homogeneous Charge Compression Ignition Engines and Their Effects on Operational and Controlling Issues. *Int. J. Engine Res.*, 2004, **5**, 297-316.
17. **Ra, Y., Hruby, E. J.,** and **Reitz, R. D.** Parametric Study of Combustion Characteristics in a Direct-Injection Diesel Homogeneous Charge Compression Ignition Engine with a Low-Pressure Fuel Injector. *Int. J. Engine Res.*, 2005, **6**, 215-230.
18. **Kook, S., Bae, C.,** and **Kim, J.** Diesel Fuelled Homogeneous Charge Compression Ignition Engine with Optimized Premixing Strategies. *Int. J. Engine Res.*, 2007, **8**, 127-137.
19. **Xu, H. M., Wyszynski, M. L., Megaritis, A., Yap, D., Wilson, T., Qiao, J., Richardson, S., Golunski, S.,** and **Peucheret, S.** Research on Expansion of Operating Windows of Controlled Homogeneous Auto-Ignition Engines. *Int. J. Engine Res.*, 2007, **8**, 29-40.
20. **Caton, P. A.,** and **Pruitt, J. T.** Homogeneous Charge Compression Ignition of Hydrogen in a Single-Cylinder Diesel Engine. *Int. J. Engine Res.*, 2009, **10**, 45-63.
21. **Yun, H., Wermuth, N.,** and **Najt, P.** High Load HCCI Operation Using Different Valving Strategies in a Naturally-Aspirated Gasoline HCCI Engine. SAE paper 2011-01-0899, 2011.
22. **Maurya, R. K. and Agarwal, A. K.** Experimental Study of Combustion and Emission Characteristics of Ethanol Fuelled Port Injected Homogeneous Charge Compression Ignition (HCCI) Combustion Engine. *Appl Energy.*, 2011, **88**, 1169-1180.
23. **Sakai, A., Takeyama, H., Ogawa, H.,** and **Miyamoto, N.** Improvements in Premixed Charge Compression Ignition Combustion and Emissions with Lower Distillation Temperature Fuels. *Int. J. Engine Res.*, 2005, **6**, 433-442.
24. **Shimazaki, N., Minato, A.,** and **Nishimura, T.** Premixed Diesel Combustion Using Direct Injection Near Top Dead Centre. *Int. J. Engine Res.*, 2007, **8**, 259-270.
25. **Nevin, R. M., Sun, Y., Gonzalez, M. A.,** and **Reitz, R. D.** PCCI Investigation Using Variable Intake Valve Closing in a Heavy Duty Diesel Engine. SAE paper 2007-01-0903, 2007.
26. **Horibe, N., Harada, S., Ishiyama, T.,** and **Shioji, M.** Improvement of Premixed Charge Compression Ignition-Based Combustion by Two-Stage Injection. *Int. J. Engine Res.*, 2009, **10**, 71-80.
27. **Kokjohn, S. L.,** and **Reitz, R. D.** Investigation of Charge Preparation Strategies for Controlled Premixed Charge Compression Ignition Combustion Using a Variable Pressure Injection System. *Int. J. Engine Res.*, 2010, **11**, 257-282.
28. **Park, Y.** and **Bae, C.** Influence of EGR and Pilot Injection on PCCI Combustion in a Single-Cylinder Diesel Engine. SAE paper 2011-01-1823, 2011.
29. **Benajes, J., Novella, R., Garcia, A., Domenech, V.,** and **Durrett, R.** An Investigation on Mixing and Auto-ignition using Diesel and Gasoline in a Direct-Injection Compression-Ignition Engine Operating in PCCI Combustion Conditions. SAE paper 2011-37-0008, 2011.
30. **Lewander, M., Johansson, B., Tunestål, P., Keeler, N., Tullis, S., Milovanovic, N.,** and **Bergstrand, P.** Evaluation of the Operating Range of Partially Premixed Combustion in a Multi Cylinder Heavy Duty Engine with Extensive EGR. SAE paper 2009-01-1127, 2009.
31. **Shi, Y., Wang, Y.,** and **Reitz, R. D.** Computational Fluid Dynamic Modelling a Heavy-Duty Compression-Ignition Engine Fuelled with Diesel and Gasoline-Like Fuels. *Int. J. Engine Res.*, 2010, **11**, 355-373.
32. **Su, W.,** and **Yu, W.** Effects of Mixing and Chemical Parameters on Thermal Efficiency in a Partly Premixed Combustion Diesel Engine with Near-Zero Emissions. *Int. J. Engine Res.*, 2012, **13**, 188-198.
33. **Valentino, G., Corcione, F. E.,** and **Iannuzzi, S. E.** Effects of Gasoline–Diesel and n-butanol–Diesel Blends on Performance and Emissions of an Automotive Direct Injection Diesel Engine. *Int. J. Engine Res.*, 2012, **13**, 199-215.
34. **Minami, T., Takeuchi, K.,** and **Shimazaki, N.** Reduction of Diesel Engine NOx Using Pilot Injection. SAE paper 950611, 1995.

35. **Han, Z., Uludogan, A. N., Hampson, G. J.,** and **Reitz, R. D.** Mechanism of Soot and NOx Emission Reduction Using Multiple-Injection in a Diesel Engine. SAE paper 960633, 1996.
36. **Farrell, P. V., Chang, C. T.,** and **Su, T. F.** High Pressure Multiple Injection Spray Characteristics. SAE paper 960860, 1996.
37. **Montgomery, D. T.** and **Reitz, R. D.** Effects of Multiple Injections and Flexible Control of Boost and EGR on Emissions and Fuel Consumption of a Heavy-Duty Diesel Engine. SAE paper 2001-01-0195, 2001.
38. **Zhang, Y., Ito, T.,** and **Nishida, K.** Characterization of Mixture Formation in Split-Injection Diesel Sprays via Laser Absorption-Scattering (LAS) Technique. SAE paper 2001-01-3498, 2001.
39. **Carlucci, P., Ficarella, A.,** and **Laforgia, D.** Effects of Pilot Injection Parameters on Combustion for Common Rail Diesel Engines. SAE paper 2003-01-0700, 2003.
40. **Carlucci, P., Ficarella, A.,** and **Laforgia, D.** Effects on Combustion and Emissions of Early and Pilot Fuel Injections in Diesel Engines. *Int. J. Engine Res.*, 2005, **6**, 43-60.
41. **Shayler, P. J., Brooks, T. D., Pugh, G. J.,** and **Gambrill, R.** The Influence of Pilot and Split-Main Injection Parameters on Diesel Emissions and Fuel Consumption. SAE paper 2005-01-0375, 2005.
42. **Koyanagi, K., Öing, H., Renner, G.,** and **Maly, R.** Optimizing Common Rail-Injection by Optical Diagnostics in a Transparent Production Type Diesel Engine. SAE paper 1999-01-3646, 1999.
43. **Badami, M., Millo, F.,** and **D'Amato, D. D.** Experimental Investigation on Soot and NOx Formation in a DI Common Rail Diesel Engine with Pilot Injection. SAE paper 2001-01-0657, 2001.
44. **Schmid, M., Leipertz, A.,** and **Fettes, C.** Influence of Nozzle Hole Geometry, Rail Pressure and Pre-Injection on Injection, Vaporisation and Combustion in a Single-Cylinder Transparent Passenger Car Common Rail Engine. SAE paper 2002-01-2665, 2002.
45. **Kook, S.** and **Bae, C.** Combustion Control Using Two-Stage Diesel Fuel Injection in a Single-Cylinder PCCI Engine. SAE paper 2004-01-0938, 2004.
46. **Horibe, N., Annen, T., Miyazaki, Y.,** and **Ishiyama, T.** Heat Release Rate and NOx Formation Process in Two-Stage Injection Diesel PCCI Combustion in a Constant-Volume Vessel. SAE paper 2010-01-0608, 2010.
47. **Bianchi, G. M., Falfari, S., Parotto, M.,** and **Osbat, G.** Advanced Modeling of Common Rail Injector Dynamics and Comparison with Experiments. SAE paper 2003-01-0006, 2003.
48. **Bianchi, G. M., Falfari, S., Brusiani, F., Pelloni, P., Osbat, G.,** and **Parotto, M.** Numerical Investigation of Critical Issues in Multiple-Injection Strategy Operated by a New C.R. Fast-Actuation Solenoid Injector. SAE paper 2005-01-1236, 2005.
49. **Pontoppidan, M., Ausiello, F., Bella, G.,** and **Ubertini, S.** Study of the Impact on the Spray Shape Stability and the Combustion Process of Supply Pressure Fluctuations in CR-Diesel Injectors. SAE paper 2004-01-0023, 2004.
50. **Beierer, P., Huhtala, K., Lehto, E.,** and **Vilenius, M.** Study of the Impact of System Characteristics on Pressure Oscillations in a Common Rail Diesel Fuel Injection System. SAE paper 2005-01-0910, 2005.
51. **Beierer, P., Huhtala, K.,** and **Vilenius, M.** Experimental Study of the Hydraulic Circuit of a Commercial Common Rail Diesel Fuel Injection System. SAE paper 2007-01-0487, 2007.
52. **Ishikawa, S., Ohmori, Y., Fukushima, S., Suzuki, T., Takamura, A.,** and **Kamimoto, T.** Measurement of Rate of Multiple-Injection in CDI Diesel Engines. SAE paper 2000-01-1257, 2000.
53. **Bower, G. R.** and **Foster, D. E.** A Comparison of the Bosch and Zuech Rate of Injection Meters. SAE paper 910724, 1991.
54. **Heywood, J. B.** *Internal Combustion Engine Fundamentals*, 1988 (McGraw-Hill Book Co., New York).

APPENDIX

Notation

Δp	change in pressure
Δt	time interval
ΔV	change in volume
γ	ratio of specific heats
k	bulk modulus

n	number of data points
p	pressure
t	time
V	volume

Abbreviations

AFR	air-fuel ratio
ATDC	after top dead centre
CAD	crank angle degree
CMOS	complementary metal–oxide semiconductor
CR	common rail
CVC	constant volume chamber
DA	dwell angle
DI	direct injection
EGR	exhaust gas recirculation
ET	energising time
FFT	fast fourier transform
FIE	fuel injection equipment
FSN	filter smoke number
FVC	first visible combustion
HCCI	homogenous charge compression ignition
HRR	heat release rate
HSDI	high-speed direct injection
IC	internal combustion
LAS	laser absorption scattering
LTC	low temperature combustion
MHRR	maximum heat release rate
NA	naturally aspirated
NOx	nitrogen oxides
PCCI	premixed charged compression ignition
PM	particulate matter
PPC	partially premixed combustion
SOFI	start of first injection
SOSI	start of second injection
TDC	top dead centre
VCO	valve covered orifice